Modeling and Online Parameter Identification of Li-Polymer Battery Cells for SOC estimation

H. Rahimi-Eichi*, F. Baronti** and M.-Y. Chow*
*Department of Electrical and Computer Engineering, North Carolina State University, NC, USA
**Department of Information Engineering, University of Pisa, Pisa, Italy
Emails: hrahimi@ncsu.edu, federico.baronti@iet.unipi.it, chow@ncsu.edu

***Abstract*—Finding an accurate and easily to implement model of batteries is an essential step in properly estimating the state of charge (SOC) of the battery in real-time. In this paper, an equivalent circuit based battery model with nonlinear relationship between the open circuit voltage (V_{OC}) and the SOC is projected into several piece-wise linear functions. Moving window Least Squares (LS) parameter identification technique is then utilized to estimate and update the parameters of the battery model in each sampling time. The continuously updated parameters are fed to a linear observer to estimate the SOC of the battery. The effectiveness of the proposed modeling and estimation approach are verified experimentally on Lithium Polymer batteries.**

***Index Terms*—Battery modeling, piece-wise linearization, parameter identification, state observer design, State-of-Charge estimation, PHEV/PEV**

I. Introduction

NOWADAYS, various fields of research are addressing the different challenges about battery as the most important energy storage device. Future advanced transportation system via Plug-In Hybrid Electric Vehicles (PHEV) and Plug-In Electric Vehicles (PEV) is not feasible without significant improvements in battery technology and battery management system [1, 2]. Moreover, battery is a critical component in the infrastructure of the rapidly evolving smart grid. In addition to efficiency and reliability, which mostly depends on the battery technology, an accurate monitoring of the battery status information is essential for an effective power management of a smart grid. The battery status information includes state of charge (SOC), state of health (SOH) and state of function (SOF) [3]. The battery SOC is defined as the percentage of the charge left in the battery divided by the battery rated capacity and SOH is a factor to evaluate the ability of the battery to repeatedly provide its rated capacity over time [4]. Several approaches have been proposed to estimate the SOC [5-7] and SOH [4, 5, 8] of a battery. Those estimation approaches are mostly based on a dynamic model of the battery. Thus, a more precise battery modeling results in a more accurate state estimation.

According to the accuracy and application different types of model have been developed for battery. Electrochemical models [8] are the conventional models that use complex electrochemical equations to describe microscopic and macroscopic behaviors of the battery. Since these equations mostly need computational and time consuming methods to be solved, they are more appropriate for battery design optimization processes. Mathematical models are other tools to describe the dynamics of the battery using statistical and empirical data. These models are more appropriate to predict efficiency or capacity of the battery and are not able to give an explicit relationship between current, voltage and temperature (measurable values of the battery) for simulation. Moreover, the mathematical models are not very accurate and usually come with 5-20% error. That is why Electrical models or RC equivalent circuits are proposed to represent the dynamics of the battery more accurately [9]. These models, although not as accurate as electrochemical models, are easy to implement and use less computational time and memory to be implemented [9]. Optimal modeling for each battery and each particular application is a trade-off between accuracy of the model and complexity and the order of the battery equations.

Despite the intrinsic nonlinear behavior of the battery, mainly caused by V_{OC}-SOC nonlinear function, a piecewise linear model for a battery is proposed in this paper. Due to the strong background theory for linear systems and convenient design tools, design and analysis in the linear area is a significant benefit. On the other hand, considering the V_{OC}-SOC curve of the lithium polymer battery obtained from experimental tests makes the piecewise linear approximation of the V_{OC}-SOC function reasonable. This verification will be discussed in details in the next section. Therefore, considering a piecewise linear relationship between V_{OC} and SOC, the battery model can be presented as a linear system transfer function with step-wise varying parameters. This structure is appropriate to apply an online parameter identification algorithm to estimate the parameters of the system that are changing with SOC. We identify the parameters of the linear system using the well-known moving window least-squares (LS) identification method. Afterwards, the identified parameters are used to update the parameters of the observer structure to estimate the SOC of the battery.

In the followings, Section II describes the components of the battery model employed in this paper; Section III explains the parameter identification algorithm and the state observer design; Section VI talks about experimental tests; Section V shows the results of applying the proposed identification and estimation approach to the experimental data; and Section VI concludes the paper.

978-1-4673-0158-9/12/$31.00 ©2012 IEEE

II. BATTERY MODELING

Different equivalent circuits have been proposed to model the dynamics of the battery. Based on the expected accuracy, different components can be added to the model to represent various characteristics of the battery. On the other side, embedding several components into the model creates a large amount of complexity and a system with a higher order. Therefore, considering the details in the model is a trade-off between accuracy and complexity. In the following, we will describe some of the battery characteristics that are considered in the battery model for this paper.

A. Linear Model with Internal Resistance

A typical battery can casually be modeled by a large capacitor. The capacitor can store a large amount of electrical energy in the charging mode and release it during discharging mode. Since this charging/discharging is a chemical process with electrolyte and inter-phase resistance, a small resistor, *R*, is considered in series with a capacitor, *C*. This small resistor is called the internal resistor of the battery and changes with the state of charge, the ambient temperature and the aging effect of the battery.

B. Relaxation Effect

Relaxation effect is another fundamental characteristic of the battery that emerges in the cycles of charging and discharging. This effect represents the slow convergence of the battery open circuit voltage (V_{OC}) to its equilibrium point after hours of relaxation following charging/discharging. Relaxation effect is a phenomenon caused by diffusion effect and double layer charging/discharging effect [9]. This characteristic is modeled by series-connected parallel RC circuits. Regarding the trade-off between accuracy and complexity, a different number of RC groups can be considered in the equivalent model. Figure 1 shows the equivalent circuit for the model that contains the relaxation effect.

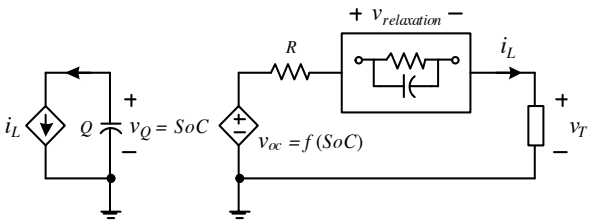

Figure 1. Combined battery model with Relaxation effect, internal resistance and V_{OC}-SOC function

Moreover, another difference between this model and the linear one is that this model has a controlled voltage source to include the nonlinear relationship between open circuit voltage and the state of charge.

C. V_{OC}-SOC relationship

The V_{OC}-SOC relationship is a static characteristic of a battery under predetermined conditions of temperature and age. To model this nonlinear part of the battery several nonlinear equations have been proposed [6]. Some of these equations also consider the hysteresis effect of the battery. The hysteresis effect, which is beyond the scope of this paper, causes the discharging curve to stay below the charging curve for the same amount of SOC. Although the proposed models for the V_{OC}-SOC function are comprehensive, fitting the experimental V_{OC}-SOC curve to the equations results in modeling errors. Moreover the nonlinearity of the model increases the complexity of the analysis regarding stability and performance of the estimators. Therefore, considering the V_{OC}-SOC curve of the lithium polymer battery from experimental results, shown in Figure 2, it gives the intuitive idea that it can be divided into several linear regions. We used the first and the second derivative of the V_{OC} versus SOC to find out if we can find proper finite linear segments for the V_{OC}-SOC curve. The first derivative ($\frac{\partial V_{OC}}{\partial SOC}$) and the second one ($\frac{\partial^2(V_{OC})}{(\partial(SOC))^2}$) are displayed in Figures (3a) and (3b) respectively.

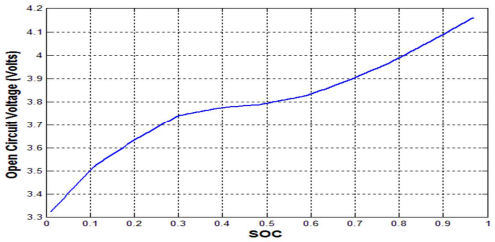

Figure 2. Actual V_{OC}-SOC curve of the Li-Polymer battery.

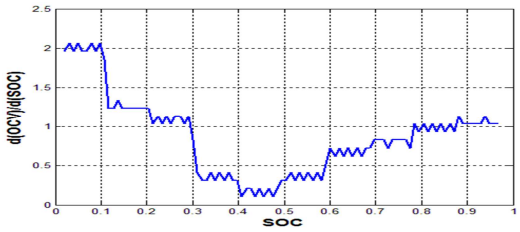

(a)

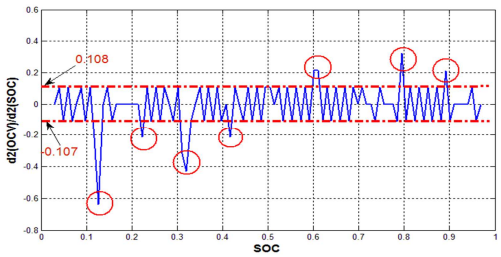

(b)

Figure 3. The first (a) and the second (b) derivative of V_{OC} versus SOC.

Figure 3b. shows that most of the second derivative values are within the small interval of [-0.107, 0.108] and a few (exactly 7) points stand out of this region. They can be considered as the cross points to divide the curve into linear segments. Therefore, as shown in Figure 4, the V_{OC}-SOC

curve is approximated by 8 segments, each of them described by the following linear equation:

$$V_{oc} = f(SOC) = b_0 + b_1 SOC. \quad (1)$$

Using least square error curve fitting technique the values for b_0 and b_1 and the goodness of fit evaluation factor, R^2, can be derived for each segment. The results, presented in TABLE I, shows that b_1 which is the slope of the mapping line starts from a large value of 1.97 for SOC<0.11, gradually decreases to the smallest value of 0.3 on the 5th segment and afterwards increases to 1.05 for SOC>0.89. Moreover, the fitting criteria, R^2, indicates that segment 5 (0.4<SOC<0.6) has the worst fitting factor compared to the other segments. Segment 4 has the next worst fitting criteria; while the first and the last segments are the best fitted ones.

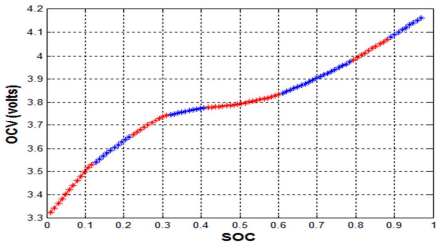

Figure 4. Piecewise Linear mapping of V_{OC}-SOC curve

TABLE I. Parameters and fitness of Piecewise linear segments

Seg.\Param.	b_0	b_1	R^2
1	3.3046	1.9702	0.9991
2	3.3861	1.2348	0.9997
3	3.4299	1.0337	0.9945
4	3.6407	0.3389	0.9933
5	3.6479	0.3014	0.9667
6	3.3746	0.7604	0.9979
7	3.1981	0.9892	0.9998
8	3.1442	1.0509	0.9999

D. State-Space Equations for the Model

To model the battery characteristics, we used an equivalent circuit like that of Figure 5 with one RC group to represent the relaxation effect. Although two RC groups are recommended by [9] as the optimal trade-off between accuracy and complexity of the model, there are also several references [4, 7, 10] that state that one RC group structure can provide accurate enough results for a short time duration (e.g., seconds to minutes) prediction such as the applications in PHEV and PEV. Therefore, we chose this simple model to reduce the complexity of the model identification and the parameter extraction. Moreover, as we discussed earlier the V_{OC} vs. SOC function is mapped to several piecewise linear equations with the form of equation (1). Considering the equivalent circuit for the battery model in Figure 5, the state-space equations can be written as system (2) to represent the battery dynamics. In these equations, the SOC of the battery, and the voltage across the RC cell, V_{RC}, are selected to be system state variables.

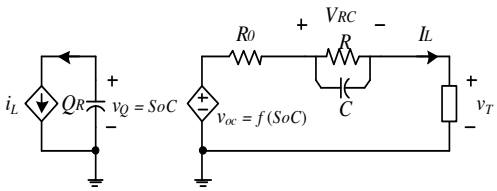

Figure 5. A battery-equivalent circuit.

$$\begin{cases} \begin{bmatrix} \dot{SOC} \\ \dot{V_{RC}} \end{bmatrix} = \begin{bmatrix} 0 & 0 \\ 0 & -\frac{1}{RC} \end{bmatrix} \begin{bmatrix} SOC \\ V_{RC} \end{bmatrix} + \begin{bmatrix} 1/Q_R \\ 1/C \end{bmatrix} I_L \\ V_T = \begin{bmatrix} b_1 & 1 \end{bmatrix} \begin{bmatrix} SOC \\ V_{RC} \end{bmatrix} + R_0 I_L + b_0 \end{cases} . \quad (2)$$

In this paper, we assume that the terminal current (I_L) and voltage (V_T) are the only two values that are accessible from system (2). In this paper, we do not consider the temperature effect and the capacity fading caused by ageing of the battery. To obtain the estimated State of Charge as one of the states, the parameters in system (2) need to be identified. Apparently, we know Q_R to be the nominal capacity of the battery. So, we need to estimate $\{b_0, R, C, R_0, b_1, S_{oc}, V_{RC}\}$ as $\{\hat{b}_0, \hat{R}, \hat{C}, \hat{R}_0, \hat{b}_1, \hat{S}_{oc}, \hat{V}_{RC}\}$ using system parameter identification methods and state estimation.

III. System Parameter Identification and State Estimation

A. Least-Squares (LS) and Recursive Least-Squares Parameter (RLS) Identification

In order to identify the parameters of a linear time-invariant (LTI) system, the relationship between the system input/ output (I/O) samples is described by a standard structure, such as the autoregressive exogenous model (ARX model) [11]:

$$A(q)y(q) = B(q)u(q) + e(q), \quad (3)$$

in which,

$$A(q) = 1 + a_1 q^{-1} + \cdots + a_n q^{-n}, \quad (4)$$

$$B(q) = b_0 + b_1 q^{-1} + \cdots + b_m q^{-m}, \quad (5)$$

and $e(q)$ is a zero mean Gaussian white noise. Therefore, with this model the output at the present step can be estimated by the input and output values at previous steps. Least Square (LS) identification approach provides a formula to minimize the least-square error between this estimated output value and the real output at present step. Since the input-output samples are being updated step-by-step while the system is running, the Recursive Least Square (RLS) is used to estimate the parameters of the system iteratively. Due to the fact that implementing the RLS algorithm is not easy in a real system and the I/O signal needs to be persistently exciting (PE) [11] at each step, we use the moving-window LS method, which is more practical. In this approach, the I/O data corresponding to a certain number of (window) past steps is used to estimate the parameters. The length of the window depends on the excitation of the input signal to properly reveal the dynamics of the system.

B. Battery Parameter Identification

The parameters of the battery model needed to be estimated consist of: $\{b_0, R, C, R_0, b_1\}$. Since most of the parameter identification methods use the transfer function of the system to identify the parameters, first we obtain the transfer function form of system (2):

$$\frac{Y(s)-b_0}{U(s)} = \frac{R_0 s^2 + \left(\frac{b_1}{Q_R}+\frac{1}{C}+\frac{R_0}{RC}\right)s + \frac{b_1}{RCQ_R}}{s\left(s+\frac{1}{RC}\right)}, \quad (5)$$

From transfer function (16) and using bilinear transform ($s \to \frac{2}{T}\frac{z-1}{z+1}$) [12], we can get the discrete transfer function of system (2) with sample time T:

$$\frac{Y(z^{-1})-b_0}{U(z^{-1})} = \frac{c_0+c_1 z^{-1}+c_2 z^{-2}}{1+a_1 z^{-1}+a_2 z^{-2}}, \quad (6)$$

where:

$$c_0 = \frac{T^2 b_1 + 2Q_R R_0 T + 2Q_R RT + 4Q_R R_0 RC + 2b_1 RCT}{2Q_R T + 4Q_R RC}, \quad (7a)$$

$$c_1 = \frac{T^2 b_1 - 4Q_R R_0 RC}{Q_R T + 2Q_R RC}, \quad (8b)$$

$$c_2 = \frac{T^2 b_1 - 2Q_R R_0 T - 2Q_R RT + 4Q_R R_0 RC - 2b_1 RCT}{2Q_R T + 4Q_R RC}, \quad (8c)$$

$$a_1 = \frac{-8Q_R RC}{2Q_R T + 4Q_R RC}, \quad (8d)$$

$$a_2 = \frac{-2Q_R T + 4Q_R RC}{2Q_R T + 4Q_R RC}. \quad (8e)$$

According to equations (7) and (8), the time-domain relationship between different samples of input and output is as follows:

$$y(k) = -a_1 y(k-1) - a_2 y(k-2) + b_0(1 + a_1 + a_2) + c_0 u(k) + c_1 u(k-1) + c_2 u(k-2). \quad (9)$$

Equations (8d) and (8e) imply that:

$$1 + a_1 + a_2 = 0, \quad (10)$$

which means that the value of b_0 does not affect the estimation of the current output $y(k)$, and subsequently, the other parameters. In other words, b_0 acts like an output offset that does not influence the dynamic between input and output. Therefore, we can show that solving equations (8a-e) gives a unique expression of the battery parameters versus the coefficients of the transfer function (7).

C. Observer Design

After identifying the parameters of the battery, an observer is designed to estimate the SOC, which is one of the states of the model. The observer compares the real output to the estimated output of the model with the identified parameters. Then, it compensates for the error, caused by uncertainties and initial values, by giving a proper feedback to the states via a designed gain (observer gain).

Thus, in this stage the battery parameters $\{R, C, R_0, b_1, b_0\}$ are assumed to be estimated as $\{\hat{R}, \hat{C}, \hat{R}_0, \hat{b}_1, \hat{b}_0\}$. Moreover, the battery model is represented as a system with equations (11):

$$\begin{cases} \dot{x} = Ax + Bu \\ y = Cx + Du + b_0 \end{cases} \quad (11)$$

in which, $x_1 = S_{oc}, x_2 = V_{RC}, A = \begin{bmatrix} 0 & 0 \\ 0 & -\frac{1}{RC} \end{bmatrix}, B = \begin{bmatrix} 1/Q_R \\ 1/C \end{bmatrix}$, $C = [b_1 \quad 1]$, $D = R_0$, $u = I_L$, $y = V_T$, $x = \begin{bmatrix} x_1 \\ x_2 \end{bmatrix}$. Therefore, the observer can be designed as a system with equations (12):

$$\begin{cases} \dot{\hat{x}} = A\hat{x} + Bu + L(y - \hat{y}) \\ \hat{y} = C\hat{x} + Du + b_0 \end{cases} \quad (12)$$

in which $L^T = [L_1 \quad L_2]$ is the observer gain vector.

Figure 6 shows the block diagram of the observer. In this diagram, the estimated terminal voltage is calculated by applying input, I_L, to a dynamic model with state space matrices of A, B, C and R_0 as D. Adding b_0 as an offset, this estimated out is subtracted from the real terminal voltage of the battery to provide the error signal. This signal is magnified by the observer gain, L to obtain the feedback to the estimated states of the battery.

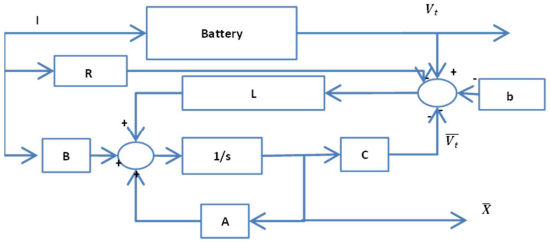

Figure 6. Observer structure

IV. Battery Tests

Actual experiments have been carried out on lithium-polymer cells to validate the above described method. The lithium-polymer battery technology was selected because of its very high energy and power densities. These characteristics, along with other positive aspects, such as the very low self-discharge rate (around 3 % per month) and the very high charge/discharge efficiency, common to other lithium-ion battery technologies, make this technology very attractive for improving the performance and the driving range of PHEVs and PEVs [13].

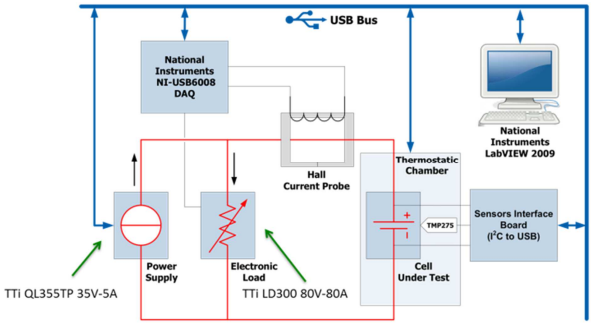

Figure 7. Schematic diagram of the experimental set-up

The tests were performed on 1.5 Ah lithium-polymer cells using the experimental set-up sketched in Figure 7. The cell under test is placed inside a custom temperature-controlled chamber, so that the cell temperature can be kept at given value during a test [13]. As shown in Figure 7, a power supply and an electronic load to be charged and discharged at the

desired current. The cell voltage and current are measured by a 16-bit ADC and an Agilent 1146A 100 kHz/100A AC/DC Hall Current Probe respectively. All the instruments are connected to a PC and managed by an application developed in LabVIEW graphical programming environment.

The cells (Kokam SLPB723870H4) used in the tests can continuously be charged and discharged within the 2.7 V and 4.2 V voltage range with currents up to 3 A and 30 A respectively. All the performed tests have the same structure, including an *Init Phase*, a *Pause Phase* and a *Test Phase*. During the *Init Phase* the cell is completely charged (continuous-current followed by continuous-voltage mode) and then, after one hour pause, is completely discharged, with the current of 1.5 A. During the *Pause* (one hour) the cell settles down ensuring that all the transients subside before starting the real test (*Test Phase*), which will thus start from a well-known status. A significant example of the *Test Phase* is the pulsed charge/discharge cycle, which makes it possible to extract valuable characteristics of the cell under test. In particular, if we consider the behavior of the cell terminal voltage during the zero current intervals and we fit it with an exponential function, the open circuit voltage at the state of charge given by the coulomb counting of the measured cell current is given by the final value of the exponential fitting. This method was applied to derive the V_{OC}-SOC curve depicted in Figure 2. For this purpose, each current pulse determined a 1 % SOC variation and the following zero current interval lasted 5 min. In fact, two V_{OC}-SOC curves could be extracted, one during the charging phase and the other during the sequent discharging phase. A small difference could be observed between the two curves, confirming that the hysteresis effect is not so evident for lithium-polymer technology, as it is for the $LiFePO_4$ lithium-ion chemistry. The curve reported in Figure 3 is the average between the charge and discharge V_{OC}-SOC curves.

V. Results and Discussion

The data acquired during the experimental tests are used to evaluate the accuracy of the piecewise linear model for the battery, the online parameter identification algorithm, and the state estimation method. Figure 8 shows the terminal current and voltage of the battery during a pulse charging of the Li-Polymer battery. These data are used as the input-output data to the moving window least square parameter identification algorithm. Since a step pulse is applied to the battery every 10 minutes (600 seconds), the moving window cannot be smaller than 300 seconds to at least include one of the pulse edges. The results for identification of the battery parameters are displayed in Figures 9a-d. We can see that in this type of battery R_0, R and C change a lot with SOC. As expected, the value for the internal resistance, R_0, is large for small SOCs and decreases when SOC increases. This frequent change verifies the essential need for online parameter identification at least in this type of battery. Moreover, the values for b_1 in figure 9d follow the expected profile for b_1 in TABLE I for a charging cycle. The relationship between b_1 and b_0, obtained from TABLE I, is demonstrated in figure 10 as a sequential diagram. This block diagram finds the corresponding b_0, which is not identifiable with parameter estimation, for each value of b_1 considering the charging sequence. The identified parameters are used to update the observer parameters with the structure of Figure 6. We use pole placement technique to assign the observer poles at appropriate values and calculate the corresponding observer

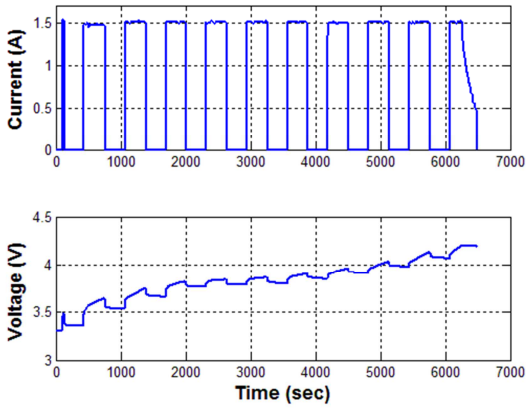

Figure 8. Current and Voltage of the battery

(a)

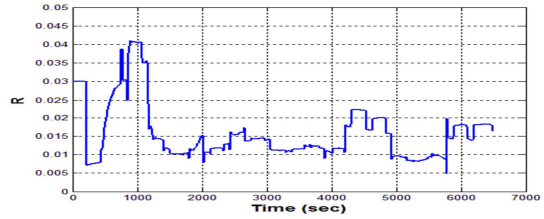

(b)

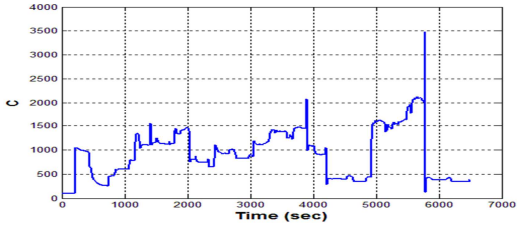

(c)

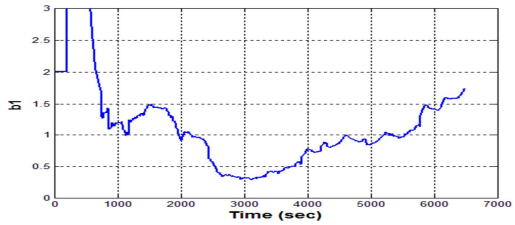

(d)

Figure 9a-d. Online identified battery parameters

gains at each step. The result for the SOC estimation is demonstrated in Figure 11. Since we know the initial SOC for this test, coulomb counting method is used to prepare a benchmark to evaluate the estimation of the observer that starts from an arbitrary initial SOC.

We can see from Figure 11 that the estimated SOC with arbitrarily chosen initial SOC follows the real value for SOC. Figure 12 shows the error in SOC estimation. We can see that most of the time the error is in the acceptable range of 5% except for the time corresponding to the SOC between 0.3 and 0.6. According to TABLE I, this range is related to segments 4 and 5 with relatively lower fitness criteria.

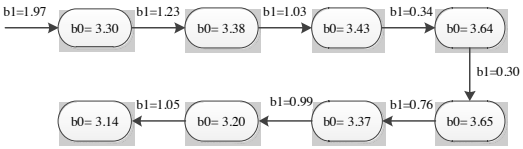

Figure 10. b_0-b_1 relationship block diagram

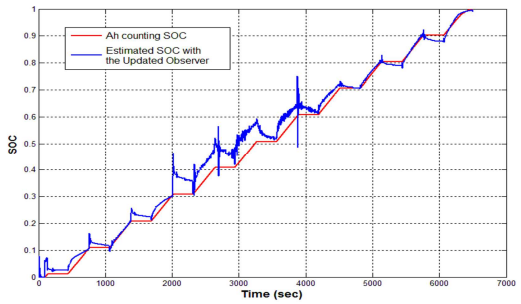

Figure11. SOC estimation result from the updating observer

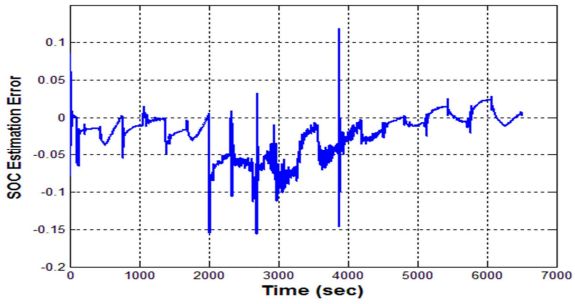

Figure12. SOC estimation error

VI. Conclusion and Future Work

Despite the inherent nonlinear dynamic of the battery mainly caused by V_{OC}-SOC relationship, a piecewise linear model is proposed for the lithium-polymer battery. The experimental curve for V_{OC}-SOC function is used to verify this assumption. The linear structure facilitates using the well-developed parameter identification and state estimation techniques in the linear systems to estimate the state of charge of the battery. Moreover, the linear structure of the estimator is easy to implement in a battery management system. Applying the estimation approach to the experimental data of the lithium-polymer battery validates the acceptability of the SOC estimation results. On the other side, the piecewise linear model for the battery has the drawback of approximation error regarding the fact that V_{OC}-SOC function is not really linear. The increase in estimation error for the nonlinear segments implies the sensitivity of the approach to nonlinearity error.

Acknowledgement

This work is partly supported by the National Science Foundation Award number: EEC-08212121.

VII. References

[1] Wencong Su, H. Eichi, Wente Zeng, and Mo-Yuen Chow, "A Survey on the Electrification of Transportation in a Smart Grid Environment," *Industrial Informatics, IEEE Transactions on,* vol. 8, pp. 1-10, 2012.

[2] S. Wencong and C. Mo-Yuen, "Sensitivity analysis on battery modeling to large-scale PHEV/PEV charging algorithms," in *IECON 2011 - 37th Annual Conference on IEEE Industrial Electronics Society*, 2011, pp. 3248-3253.

[3] Z. Hanlei and C. Mo-Yuen, "On-line PHEV battery hysteresis effect dynamics modeling," in *IECON 2010 - 36th Annual Conference of IEEE Industrial Electronics, 7-10 Nov. 2010*, Piscataway, NJ, USA, 2010, pp. 1844-9.

[4] C. R. Gould, C. M. Bingham, D. A. Stone, and P. Bentley, "New battery model and state-of-health determination through subspace parameter estimation and state-observer techniques," *IEEE Transactions on Vehicular Technology,* vol. 58, pp. 3905-16, 2009.

[5] F. Huet, "A review of impedance measurements for determination of the state-of-charge or state-of-health of secondary batteries," *Journal of Power Sources,* vol. 70, pp. 59-69, 1998.

[6] G. L. Plett, "Extended Kalman filtering for battery management systems of LiPB-based HEV battery packs - Part 2. Modeling and identification," *Journal of Power Sources,* vol. 134, pp. 262-276, 2004.

[7] M. A. Roscher and D. U. Sauer, "Dynamic electric behavior and open-circuit-voltage modeling of LiFePO4-based lithium ion secondary batteries," *Journal of Power Sources,* vol. 196, pp. 331-336, 2011.

[8] D. W. Dees, V. S. Battaglia, and A. Bélanger, "Electrochemical modeling of lithium polymer batteries," *Journal of Power Sources,* vol. 110, pp. 310-320, 2002.

[9] C. Min and G. A. Rincon-Mora, "Accurate electrical battery model capable of predicting runtime and I-V performance," *Energy Conversion, IEEE Transactions on,* vol. 21, pp. 504-511, 2006.

[10] I.-S. Kim, "A technique for estimating the state of health of lithium batteries through a dual-sliding-mode observer," *IEEE Transactions on Power Electronics,* vol. 25, pp. 1013-1022, 2010.

[11] K. J. Astrom and B. Wittenmark, *Adaptive Control*, 2 ed.: Prentice Hall, 1994.

[12] K. Ogatta, *Discrete-Time Control Systems*, 2 ed. N. J.: Prentice Hall, 1995.

[13] F. Baronti, G. Fantechi, E. Leonardi, R. Roncella, and R. Saletti, "Enhanced model for Lithium-Polymer cells including temperature effects," in *IECON 2010 - 36th Annual Conference on IEEE Industrial Electronics Society*, 2010, pp. 2329-2333.